Jeffrey, S. W. & Humphrey, G. F. 1975. New spectrophotometric equations for determining chlorophylls *a*, *b*, c_1 and c_2 in higher plants, algae and natural phytoplankton. *Biochem. Physiol. Pflanzen.* 167:191–4.

Littler, M. M., Littler, D. S. & Taylor, P. R. 1987. Functional similarity among isomorphic life-history phases of *Polycavernosa debilis* (Rhodophyta, Gracilariaceae). *J. Phycol.* 23:501–5.

Mathieson, A. C. & Burns, R. L. 1971. Ecological studies of economic red algae. I. Photosynthesis and respiration of *Chondrus crispus* Stackhouse and *Gigatina stellata* (Stackhouse) Batters. *J. Exp. Mar. Biol. Ecol.* 7:197–206.

——— 1975. Ecological studies of red algae. V. Growth and reproduction of natural and harvested populations of *Chondrus crispus* Stackhouse in New Hampshire. *J. Exp. Mar. Biol. Ecol.* 17:137–56.

Mathieson, A. C. & Norall, T. L. 1975. Physiological studies of subtidal red algae. *J. Exp. Mar. Biol. Ecol.* 20:237–47.

May, G. 1986. Life history variation in a predominantly gametophytic population of *Iridaea cordata* (Gigartinaceae, Rhodophyta). *J. Phycol.* 22:448–55.

Monterey Bay Aquarium. 1989–1990. *Monthly Weather Summary.* Monterey Bay Aquarium, Monterey, California.

Peckol, P., Harlin, M. M. & Krumscheid, P. 1988. Physiological and population ecology of intertidal and subtidal *Ascophyllum nodosum* (Phaeophyta). *J. Phycol.* 24:192–8.

Sideman, E. J. & Mathieson, A. C. 1983. Ecological and genecological distinctions of a high intertidal dwarf form of *Fucus distichus* (L.) Powell in New England. *J. Exp. Mar. Biol. Ecol.* 72:171–88.

Smith, C. M. & Berry, J. A. 1986. Recovery of photosynthesis after exposure of intertidal algae to osmotic and temperature stress: comparative studies of species with differing distributional limits. *Oecologia* 70:6–12.

Smith, D. C. & Molesworth, S. 1973. Lichen physiology. XIII. Effect of rewetting dry lichens. *New Phytol.* 72:525–33.

Sokal, R. R. & Rohlf, F. J. 1981. *Biometry*, 2nd ed. W. H. Freeman, San Francisco, 859 pp.

Stuart, T. S. 1968. Revival of respiration and photosynthesis in dried leaves of *Polypodium polypodioides*. *Planta (Berl.)* 83:185–206.

Whittick, A. 1978. The life history of *Callithamnion corymbosum* (Rhodophyta: Cermiaceae) in Newfoundland. *Can. J. Bot.* 56: 2497–9.

Woodward, D. L. 1988. Unbalanced gametophyte : sporophyte ratios in populations of the intertidal red alga *Endocladia muricata* in central California. Ph.D. Thesis, University of California, Los Angeles, 179 pp.

J. Phycol. **29,** 745–755 (1993)

ANTARCTIC CYANOBACTERIA: LIGHT, NUTRIENTS, AND PHOTOSYNTHESIS IN THE MICROBIAL MAT ENVIRONMENT[1]

Warwick F. Vincent[2]

Département de biologie, Université Laval, Sainte Foy, Québec, Canada G1K 7P4

Richard W. Castenholz

Department of Biology, University of Oregon, Eugene, Oregon 97403

and

Malcolm T. Downes and Clive Howard-Williams

National Institute of Water and Atmospheric Research Limited, P.O. Box 8602, Christchurch, New Zealand

ABSTRACT

The microenvironmental and photosynthetic characteristics of Antarctic microbial mats were measured in a series of ponds near McMurdo Sound. As elsewhere in Antarctica, these cold-water benthic communities were dominated by oscillatoriacean cyanobacteria. Despite large variations in mat thickness, surface morphology, and color, all of the communities had a similar pigment organization, with a surface carotenoid-rich layer that overlaid a deep chlorophyll maximum (DCM) enriched in phycocyanin as well as chlorophyll a. *Spectroradiometric analyses showed that the DCM population inhabited an orange-red shade environment. In several of the mats, the deep-living trichomes migrated up to the surface of the mat within 2 h in response to a 10-fold decrease in surface irradiance. The euphotic layer of the mats was supersaturated in oxygen and contained ammonium and dissolved reactive phosphorus concentrations in excess of 100 mg* $N \cdot m^{-3}$ *or* $P \cdot m^{-3}$. *Integral photosynthesis by core samples was saturated at low irradiances and varied two- to threefold throughout the continuous 24-h radiation cycle. Oxygen microelectrode analyses showed that the photosynthetic rates were slow to negligible near the surface and maximal in the DCM. These compressed, nutrient-rich euphotic zones have some properties analogous to planktonic systems, but the integrated photosynthetic responses of the community reflect the strong self-shading within the mat and physiological dominance by the motile, DCM populations.*

Key index words: Antarctica; cyanobacteria; microbial mats; Oscillatoria *spp.; photosynthesis*

[1] Received 3 March 1993. Accepted 28 July 1993.

[2] Address for reprint requests.

Mat-forming cyanobacteria are a major component of the benthic community in many freshwater environments and some intertidal, subtidal, and hypersaline marine habitats. Genera such as *Oscillatoria, Phormidium, Lyngbya, Microcoleus, Schizothrix, Calothrix, Tolypothrix,* and *Scytonema* commonly occur in the periphyton of streams, lakes, and ephemeral ponds, where they bind together the silt and sand particles to produce a cohesive, sometimes mucilage-rich layer. Certain of these mat-forming species achieve their highest natural abundance under extreme conditions of high pH, salinity, or temperature where the grazing pressure on the community is substantially reduced or eliminated (e.g. Garrett 1970, Cohen et al. 1984, Palmisano et al. 1989).

Cyanobacteria are often the dominant photosynthetic organisms in the lakes, ponds, and streams of Antarctica. These cold-water environments are fed by melting snow or glacial ice in summer and are widespread along the continental margin and offshore islands. The cyanobacteria form benthic crusts, films, and mats up to several centimeters thick that may completely envelop the bottom substrate. Large standing stocks of benthic cyanobacteria have been reported from the lakes of Signy Island (60° S, 45° W; Priddle 1980); flowing waters on James Ross Island (64° S, 58° W; Hawes and Brazier 1991); aquatic and semiaquatic habitats in the Vestfold Hills (68° S, 78° E; Broady 1986); freshwater environments along the Prince Olav Coast (69° S, 39° W; Oguni et al. 1987); lakes, ponds, and streams on Ross Island (77° S, 166° E; Broady and Kibblewhite 1991); fresh and saline waters throughout southern Victoria Land including the permanently ice-capped lakes of the McMurdo Dry Valleys (77° S, 163° E; Wharton et al. 1983, Vincent 1988); and the extensive ablation zone on the McMurdo Ice Shelf (78° S, 166° E; Howard-Williams et al. 1990).

Although cyanobacteria are highly successful in the Antarctic environment, there have been few attempts to examine their photosynthetic properties. Goldman et al. (1963) noted the bright red and orange surface pigmentation of the oscillatoriacean mats in Ross Island ponds and suggested that carotenoids might be an effective protective screen against continuous bright light during the polar summer. Their work on ice-free planktonic systems showed that photosynthesis was completely out of phase with the daily irradiance cycle, which led them to conclude that photoinhibition may play a major role in the 24-h production dynamics of polar aquatic systems.

An inverse relationship between photosynthetic capacity and incident light has also been observed over the daily cycle in the Antarctic Ocean. Populations of marine phytoplankton at latitude 78° S showed a strong reduction in photosynthesis around midday with maximal rates around 2400 (Rivkin and Putt 1987). Observations from Antarctic stream environments, however, suggested that the cyanobacterial mat communities may be much less sensitive to the daily extremes of irradiance (Howard-Williams and Vincent 1989).

The present study was undertaken to examine the physical and chemical gradients within Antarctic microbial mats and the interactions between the cyanobacteria and their solar radiation field. Our specific objectives were to determine how these compressed photosynthetic environments are structured and to measure and compare the integrated (area-specific) versus depth-specific responses of the mat communities to the ambient light regime during the period of summer meltout.

MATERIALS AND METHODS

Sampling and field measurements were conducted in the McMurdo Sound region (78° S, 164° E) at two coastal ponds on Ross Island (ponds at Cape Royds, as described by Goldman et al. 1972); in lakes, ponds, and streams in the Dry Valleys of southern Victoria Land (Fryxell Stream in the Taylor Valley and in a lake, pond, and stream in the Victoria Valley; details in Webster et al. 1994); and in a series of ponds within the McMurdo Ice Shelf albation zone (MIS). The latter is a 1500-km² region of meltwater streams and ponds in the western sector of the McMurdo Ice Shelf (details in Vincent 1988). The MIS ponds sampled during the present study were located in the undulating ice (Fresh, Conophyton, Skua, Orange, Salt, SOS, and Brack ponds as described in Howard-Williams et al. 1989) or the pinnacle ice (Pinnacle Pond). All of the MIS ponds lay within 3 km of Bratina Island (78° S, 163° W). The fieldwork was undertaken in 1989/1990 during the late summer period (December–January) of maximum meltwater production. Each mat community was assigned a code that included reference to its collection site (Table 1). The conductivity of the water overlying each of the communities was measured with a Hanna combined temperature and conductivity probe and is given in Table 1.

Dissolved oxygen and nutrients. Sections of mat and underlying sediment, approximately 100 cm² in area and 2–3 cm deep, were cut from the edge zone (10–25 cm water depth) of various ponds and submerged in a shallow tray containing surface pond water. The dissolved oxygen profile within the mat was then immediately measured with a mini-electrode (oxygen needle electrode Model 760 from Diamond Electro-Tech Ltd., Ann Arbor, Michigan) that was connected to a Keithley Model 845 autoranging picoammeter and referenced against a calomel electrode. The mini-electrode was linearly calibrated as in Jorgensen et al. (1983) by immersing its tip in well-stirred, surface pond water (100% saturation) or in the deeper, anaerobic layer of certain benthic mats (0% oxygen).

After each oxygen profile was completed, a second 100-cm² mat sample was obtained, immediately drained of surface water, and then split into upper (0–1 cm) and lower (1–2 cm) sections. The two layers were placed into separate Zip-lock polyethylene bags that had been washed three times with distilled water and three times with surface pond water. The bags containing the mats were laid on a flat surface, and then pressure was applied from above. A 1–4-mL subsample of the expressed interstitial water was pipetted from the bag and filtered through washed GF/C glass-fiber filters; the filtrates were then stored frozen until later analysis. Samples were also obtained from the overlying pond water on the same date of mat analysis and were similarly filtered and frozen. Additional sample blanks of pond water dispensed into the Zip-lock bags without the microbial mats were used to check for contamination.

Dissolved reactive nutrients were subsequently measured on the thawed filtrates using a Technicon II AutoAnalyser system. The nitrate plus nitrite concentrations were determined using an automated cadmium column method with Tris–ammonium chloride buffer modified from Nydahl (1976). Nitrite was quan-

TABLE 1. *Description of the mat communities sampled in the McMurdo Sound region, Antarctica, and conductivity of the lake, pond, or stream at the time of sampling. For each of the MIS and Ross Island communities, the mat code includes reference to the specific site.*

Code	Site	Conductivity ($mS \cdot cm^{-1}$)	Surface color	Thickness (mm)
Benthic mats				
O1–Fryxell	Fryxell Stream	0.02	Pink	1–4
O2–Fryxell	Fryxell Stream	0.03	Orange	2–5
O3–Victoria	Lake Victoria	0.10	Pink	2–4
O4–Victoria	Victoria Stream	0.10	Pink	2–4
O5–Pinnacle	MIS pond	0.48	Gray	1–2
O6–Fresh	MIS pond	0.55	Gray-Pink	3–4
O7–Conophyton	MIS pond	0.81	Orange	2–4
O8–Skua	MIS pond	1.54	Pink	3–5
O9–Victoria	Dry Valley pond	1.98	Orange	3–5
O10–Orange	MIS pond	3.19	Orange	2–3
S2–Salt	MIS pond	67.10	Dull green	5–20
S3–SOS	MIS pond	113.50	Dull green	5–20
Lift-off mats				
L1–P7	Ross Island pond	1.09	Orange	10–20
L2–Green	Ross Island pond	8.95	Pink	10–30
L3–Brack	MIS pond	11.60	Orange	5–15

titated by the same method but without the cadmium reduction step. The higher concentration samples were diluted with milli-Q water before final analysis. Dissolved reactive phosphorus (DRP) was measured by the autoanalytical method of Downes (1978) modified by eliminating the metabisulfite–thiosulfite reagent. Ammonium was measured by an automated version of the phenolhypochlorite method of Solorzano (1969). Urea was measured by the diacetyl monoxime method of Aminot and Kerouel (1982).

Light measurement. The penetration of downwelling irradiance through the cyanobacterial mats was measured with a LiCor 1800 scanning spectroradiometer. At each sampling time, the instrument was first set to record sky radiation over the calibrated range 300–1100 nm, at 2-nm intervals. Sections of freshly collected mat (ca. 2 cm diameter) were then laid over the 1-cm-diameter detector and scanned, followed by a repeat sky radiation measurement. The mat samples were either full-profile cores, individual layers, or cores minus specific layers. The mats were sectioned in the field with a broad, flat razor blade, and the separations were made at the junction between different-colored layers. This sectioning was done immediately prior to the spectroradiometric scan. Downwelling sky irradiance in the waveband 400–700 nm was monitored throughout the photosynthetic incubations with a LiCor cosine-corrected sensor connected to a LiCor 1600 data logger.

Pigment extraction and analysis. Cores of 10 mm diameter were cut from representative sections of mat with a plastic tube and stored in the dark at 0° C until transfer to a freezer 2–8 h later. The cores were maintained frozen at −20° C for 2–8 weeks until extraction and analysis.

They were subsequently ground in 5 mL of 90% acetone (10% water) with a Teflon tissue grinder, diluted with an additional 5 mL of 90% acetone, and then sonicated for 5 min in a Cole Parmer Ultrasonic bath (Model 8845-4). The samples were left to extract in the dark at 4° C for 4 h. At the end of this period, the extracts were vortexed or inverted and then cleared by centrifugation followed by positive-pressure filtration through a Whatman GF/F glass-fiber filter.

Subsamples of extract were injected into a Shimadzu high performance liquid chromatograph (HPLC) with a reverse-phase column and a binary solvent gradient. The initial solvent (solvent A) was 85% methanol/15% 0.175 M ammonium acetate buffer in distilled water, with a linear gradient of 90% acetone/10% water (solvent B) at 10% per minute over the first 10 min. Solvent B (100%) then continued for a further 20 min. Further details of this system are presented in Vincent et al. (1993). Subsamples for pigment identification were separated on the same HPLC system coupled to a Shimadzu SPD-M6A photodiode array detector. Where possible, the peaks were identified with standards or by their spectral characteristics determined by the photodiode array. The pigment peak areas were converted to concentrations using standards (chlorophyll *a* [Chl *a*], β-carotene) or the published extinction coefficients for identified peaks. The unidentified carotenoid peaks were converted to concentrations using the average carotenoid-specific absorption coefficient (α_{440nm}) in Mantoura and Llewellyn (1983) of 200 $L \cdot g^{-1} \cdot cm^{-1}$. The values were summed to give an estimate of total carotenoid concentration.

Photosynthesis. Three methods were used to measure photosynthetic rates. The 24-h variation in photosynthetic rates was measured by ^{14}C-bicarbonate assays of 2-mm-diameter microcores, sampled as in Vincent and Howard-Williams (1989). This size of core is a compromise between maintaining some structural integrity of the mat and maximizing the exchange of internal and external inorganic carbon pools. The cores were placed in thin-walled glass vials with freshly collected pond water and incubated *in situ* for ca. 4 h. At the end of the incubation, the cores were washed in several changes of pond water, injected with glutaraldehyde (2%) to prevent any respiratory loss of label, and stored frozen. The cores were subsequently ground in Brays scintillation cocktail with a Teflon tissue grinder, subsampled, and counted by liquid scintillation spectrometry. Dark-bottle incubations were run in parallel, and the resultant values (always less than 15% of the light bottle) were subtracted from the light fixation rates.

Samples of the pond water were collected at each incubation time for dissolved inorganic carbon measurement. The samples were acidified, and the resultant CO_2 was then passed through a Binos portable infrared gas analyzer that was calibrated at each sampling time with ampoulated sodium bicarbonate standards.

Photosynthesis versus light curves were obtained in the field with a differential infrared gas analyzer system as described by Vincent and Howard-Williams (1986). Three cores (25 mm diameter) were placed in a thin-walled glass Universal vial in a water bath maintained at 5° C. The samples were incubated under natural sunlight screened by a variable number of layers of grey Nylon shade mesh. The downwelling irradiance inside the incubation system was measured with a cosine-corrected probe. The saturating exponential model of Webb et al. (1974)—$P = P_{max}(1 - \exp(-\alpha I/P_{max}))$, where P is the photosynthetic rate normalized to Chl *a* at a specific irradiance I, α is the initial slope of the P versus I curve, and P_{max} is the maximum photosynthetic rate—was fitted to each data set by nonlinear regression. The light saturation parameter I_k was calculated as P_{max}/α.

In situ profiles of oxygen and gross photosynthetic oxygen production rates were measured with a Clark-type microelectrode that had a built-in reference and a sensing tip of about 5 μm, as

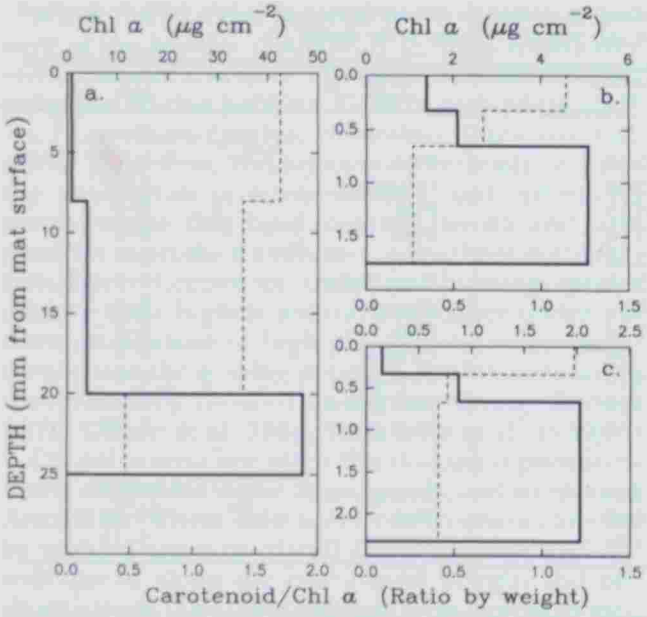

FIG. 1. Pigment distribution in three oscillatoriacean mats. The solid line is Chl *a*, and the dashed line is the carotenoid-to-Chl *a* ratio. The measurements extended to the bottom of the blue-green layer of each mat. a) L2–Green; b) O1–Fryxell; c) O10–Orange.

described in Castenholz et al. (1990). The electrode was attached to a micromanipulator, and its initial positioning at the mat-surface was determined with a magnifying telescope. Photosynthetic rates were calculated from the rates of O_2 depletion immediately following a shift from light to dark after steady-state oxygen conditions had been reached in the light.

RESULTS

Pigment Organization

Although the communities varied considerably in surface color, morphology, and mat thickness (Table 1), they shared a number of features in common. All of the cyanobacterial communities were dominated by *Phormidium* and *Oscillatoria* species (sensu Geitler 1932) with trichome diameters that ranged from 0.5 to 8 μm. They were embedded within a cohesive, mucilaginous matrix that formed a 1–4-mm-thick layer over the sediments ("benthic mats") or a 5–30-mm-thick floating layer at the surface and edge of certain ponds ("lift-off mats").

In the majority of both types of oscillatoriacean mat, there was a high degree of vertical color zonation. The surface layer of the mats was typically red or orange, except where very high concentrations of mucilage-bound sediment gave the mats a brown or gray-green appearance (e.g. O6–Fresh). The surface stratum of the mats was invariably underlaid by a blue-green layer.

Chl *a* and 6–10 carotenoid peaks (details in Vincent et al. 1993) were resolved by HPLC analysis of the lipophilic pigment extracts. In all of these oscillatoriacean mats, most of the Chl *a* was located in the blue-green layer well below the upper mat surface. This lower layer also contained the highest concentrations of total carotenoid; however, the ratio of carotenoid to Chl *a* was maximal in the surface layer (Fig. 1).

Vertical Migration

Trichome motility was a striking feature of several of the oscillatoriaceans, particularly the thicker trichome species. Cores of mat from Skua Pond (O8–Skua) visibly darkened over an 8-h period of incubation in dim light (ca. 5% ambient irradiance). Qualitative microscopic observations of surface scrapings of this mat showed that this change in color was associated with an increased near-surface abundance of trichomes of the deeper living oscillatoriaceans. When the mat in Salt Pond (S2–Salt) was covered with a 10% neutral density filter, the surface color of the mat changed from orange-brown to blue-green within 2 h. Surface scrapings of this mat provided qualitative evidence that this color change was associated with an increase in the population density of dark blue-green trichomes of *Oscillatoria priestleyi* West & West. There was no change in surface coloration of adjacent control sections of mat where plastic filter supports containing no filter were placed or under filters that transmitted ca. 25% irradiance. In these treatments, the blue-green trichomes remained below the mat surface. This type of experiment was repeated on the oscillatoriacean mats in two other ponds on the McMurdo Ice Shelf (Ice Ridge and Shading Pond), and similar results were obtained.

Dissolved Oxygen and Nutrients

In the benthic oscillatoriacean mats, the dissolved oxygen concentrations were close to equilibrium with the overlying pond water at their surface, but the values increased toward the blue-green layer, rising to a maximum that was 120–170% of air-equilibrium values (Fig. 2). The concentrations then fell with increasing depth in the profile. For several of the thicker (>10 mm) benthic mats, anoxic conditions occurred within 5–10 mm of the upper surface. The floating lift-off mat sampled from Brack Pond (L3–Brack) had oxygen concentrations in the range of 100–140% throughout its 10-mm profile.

The concentration of nutrients was one to two orders of magnitude higher in the mats than in the overlying pond water. Both ammonium and DRP sharply increased between the overlying environment and the interstitial water in the upper 10 mm of the mat (Fig. 2). In two mats sampled with anoxic bottom layers, the concentration of ammonium and DRP further increased in the 10–20-mm section of the profiles (Fig. 2). For the entire Brack Pond lift-off mat, the concentrations were similarly high: 270 mg NH_4-N·m^{-3} and 300 mg DRP·m^{-3}, in comparison to 9 mg NH_4-N·m^{-3} and 29 mg DRP·m^{-3} in the ambient pond water.

Dissolved urea (or a substance that reacted similarly with the monoxime reagent) was also measured

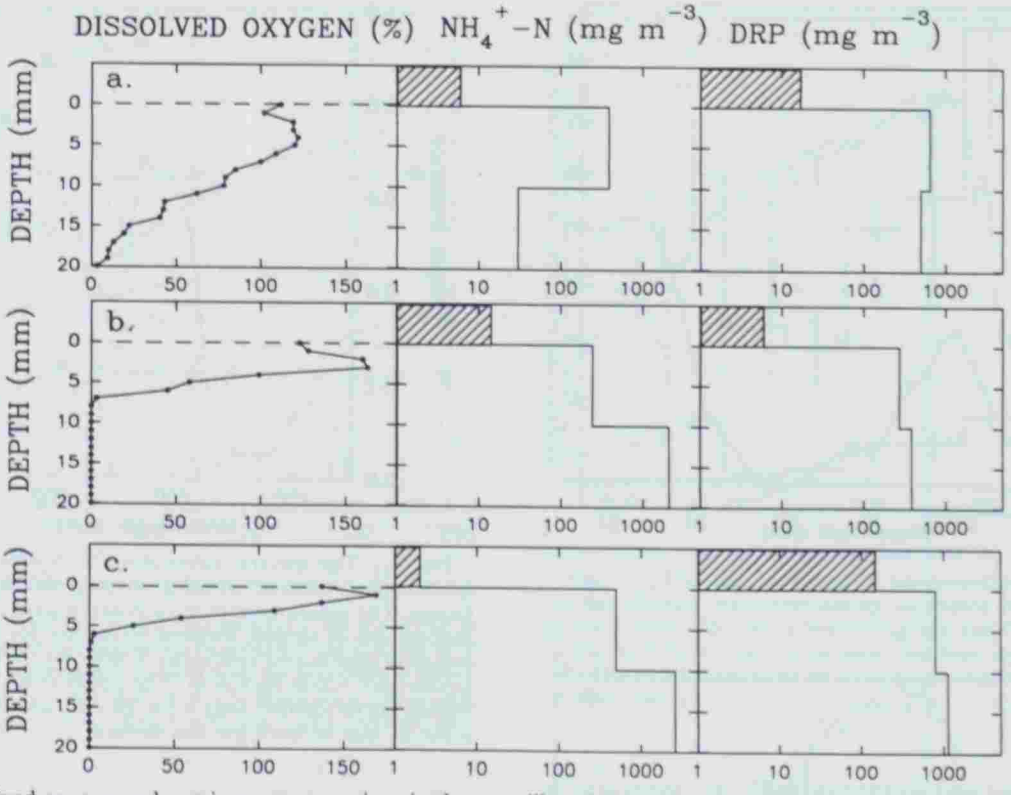

FIG. 2. Dissolved oxygen and nutrient concentrations in three oscillatoriacean mats. The dots mark the position of specific oxygen measurements down the profile. The solid lines for NH_4^+-N and DRP show the concentrations in the upper and lower sections of the mats (note the log scale). Nutrient concentrations are also given for the overlying pond water (hatched bar). Depth refers to the distance below the upper mat surface, marked by the dashed line in the oxygen profiles. Sampling was on 26 January 1990 under clear sky conditions. a) O6–Fresh; b) O7–Conophyton; c) O8–Skua.

in high concentration in the interstitial waters. The values ranged from 40 to 1640 mg $N \cdot m^{-3}$ in the interstitial waters, in comparison to 7–11 mg $N \cdot m^{-3}$ in the ponds. Nitrate concentrations were often at or near our limits of detection in the pond waters (0.6 mg $N \cdot m^{-3}$). In the mats, nitrate concentrations lay in the range of 7–15 mg $N \cdot m^{-3}$.

Spectral Irradiance Distribution

Although each of the sampled mats had its own distinctive absorption characteristics, a number of features were common to most of the spectroradiometric scans. Strongest absorption occurred in the ultraviolet and blue end of the spectrum (300–500 nm), with deepest penetration of wavelengths in the orange-red region at 600–650 nm and the infrared waveband at 750–1100 nm (Figs. 3, 4). A distinct minimum in transmitted light due to the Chl *a* absorbance maximum was often observed around 680 nm, with a second minimum at 620 nm associated with phycocyanin absorbance. There was never an absorbance maximum in the range of 500–600 nm that could be attributed to phycoerythrin (see e.g. the middle curve for L2–Green in Figs. 3b, 4). A series of spectrophotometric assays of sonicated, freshly collected oscillatoriacean mats from the McMurdo Ice Shelf ponds (specifically O10–Orange, L3–Brack, and S2–Salt) confirmed the presence of phycocyanin and absence of phycoerythrin.

The scans of individual strata of the mats indicated a high degree of spectral partitioning down through the community. In O10–Orange, for example, the upper 300 μm of the mat reduced the ultraviolet (UV)-A waveband by 70% (400 nm) to 95% (330 nm), whereas far red (700 nm) visible light was reduced by less than 50% (Fig. 3a). At the base of the mat, the visible radiation was almost completely extinguished except for a small amount in the waveband at 570–650 nm.

These spectral effects were especially well illustrated within the thicker lift-off mats. In L2–Green (Figs. 3b, 4) UV and blue wavelengths at the base of the 8-mm pink surface layer were reduced to 10% or less of the incident surface radiation, whereas 25–60% of the light at wavelengths greater than 550 nm continued to penetrate through the mat. At 20-mm depth, the depth of the interface between the orange layer and the blue-green layer, visible light was restricted to the waveband at 570–670 nm (about 2% of surface), but 5–12% of the surface infrared continued to penetrate. At the base of the mat (25 mm; bottom curve in Fig. 4), there was no detectable light in the 400–700-nm waveband, and infrared radiation was also substantially attenuated,

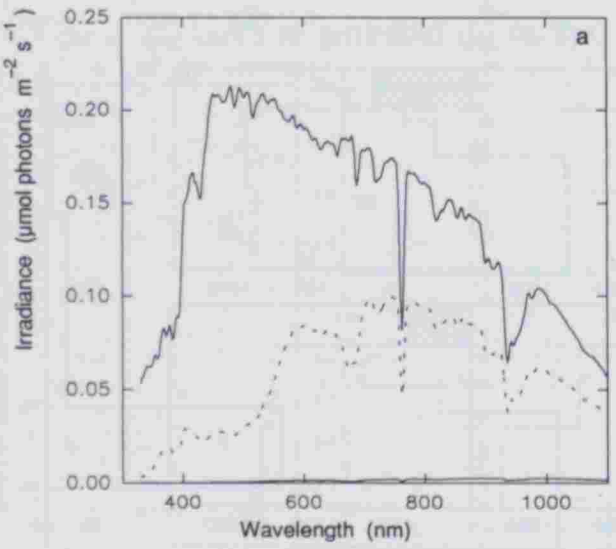

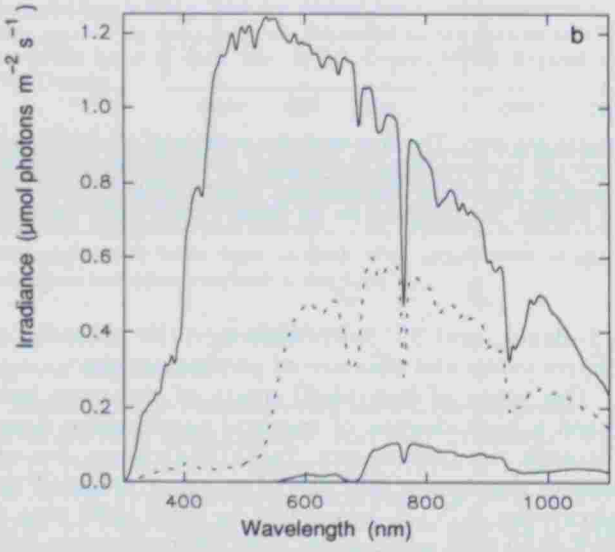

FIG. 3. The spectral attenuation of downwelling irradiance (photon fluence rate) within two types of oscillatoriacean mat communities. a) O10–Orange. Curves indicate incident radiation at the mat surface (top), 0.3 mm (middle) beneath the mat surface, and at the base of the mat (bottom) at 2 mm depth. b) L2–Green. Curves indicate incident radiation at the mat surface (top), 5 mm (middle) beneath the mat surface, and at the base of the mat (bottom) at 20 mm depth.

to 0.6% or less. The pronounced trough in the light penetration curves at 980 nm probably represents a bacteriochlorophyll–protein complex but does not correspond to any known absorption maximum of bacteriochlorophyll *a* or *b*. The lesser minima at 800 and 880 nm were probably due to bacteriochlorophyll *a*. These troughs were matched by the reddish pink strata and flecks of *Thiocapsa*-like purple bacteria, presumably sulfide-utilizing types. There was no evidence of the light-harvesting bacteriochlorophylls of the Chlorobiaceae or Chloroflexacae (i.e.

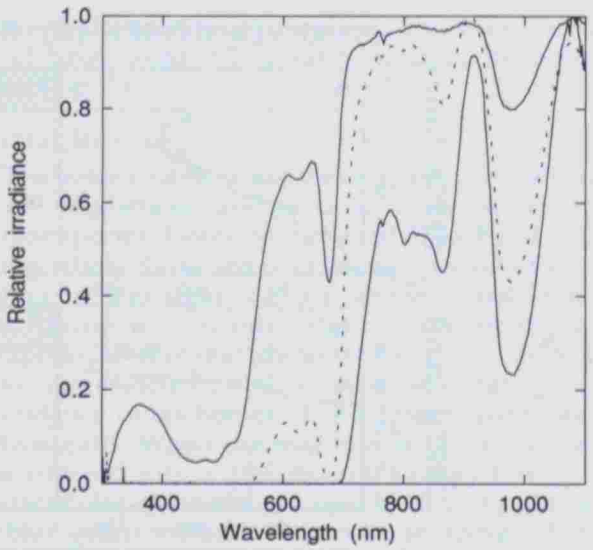

FIG. 4. The spectral attenuation of downwelling irradiance (photon fluence rate) within the thick mucilaginous mat L2–Green. The measurements at each depth were first converted to percentages of surface incident irradiance for each wavelength and were then normalized to the % value for the most penetrating wavelength within each scan. The upper curve is for 5 mm, the middle curve (dashed line) is for 20 mm, and the bottom curve is for 25 mm beneath the mat surface.

maxima in the range of 705–755 nm) in any of our spectral scans.

A comparison of attenuation coefficients for the surface and bottom layers of a representative benthic and lift-off mat further emphasized the vertical differentiation in their light-absorption properties (Table 2). Absorption within the Chl *a* waveband (K_{680}) was much higher in the bottom layer. The ratio of the attenuation coefficient at specific UV and visible wavelengths to that at 680 nm (K_{680}) showed that the highest absorbance per millimeter in the upper region of the mats was in the UV-A region (R_{350} in Table 2) and in the region of strong carotenoid absorbance (R_{480}). The bottom layers absorbed more uniformly across the visible waveband, but the relative absorption of UV wavelengths was reduced.

TABLE 2. *Spectroradiometric absorbance measurements in the surface and bottom layers of representative mat communities. The attenuation ratio (R) is the diffuse attenuation coefficient for downwelling irradiance at the specified wavelength divided by that at 680 nm (K_{680}). Section refers to the thickness (mm) of the upper (U) or lower (L) strata that were sampled.*

Code	Section	K_{680} (mm^{-1})	Attenuation ratio			
			R_{350}	R_{480}	R_{560}	R_{620}
O7–Conophyton	U2	1.3	1.47	1.87	0.86	0.68
O7–Conophyton	L2	3.7	0.78	1.06	1.03	0.98
L3–Brack	U5	0.5	1.75	1.77	0.93	0.83
L3–Brack	L7	1.3	0.63	0.99	0.83	0.94

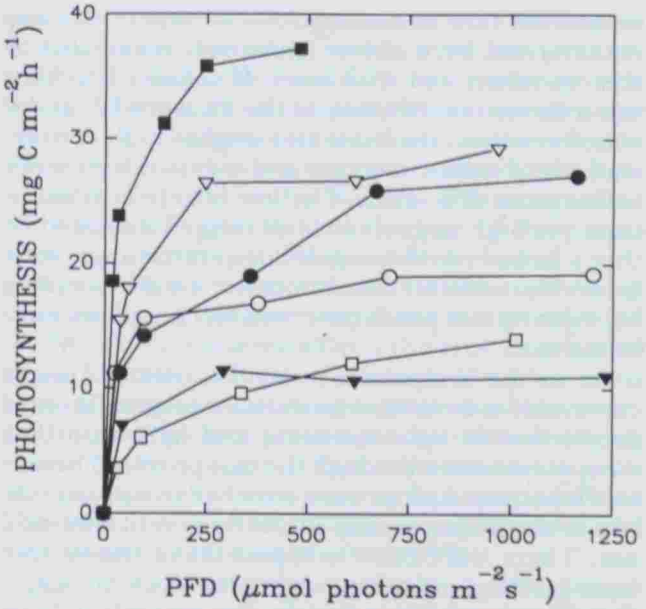

FIG. 5. Photosynthesis versus irradiance curves for cores of several mat communities measured by infrared gas analysis at 5° C and incubated under ambient light with neutral density filters, 24 January 1990. □ = S3–SOS, ▼ = L3–Brack, ○ = O6–Fresh, ● = O10–Orange, ▽ = L3–Brack with the cores inverted, ■ = O8–Skua.

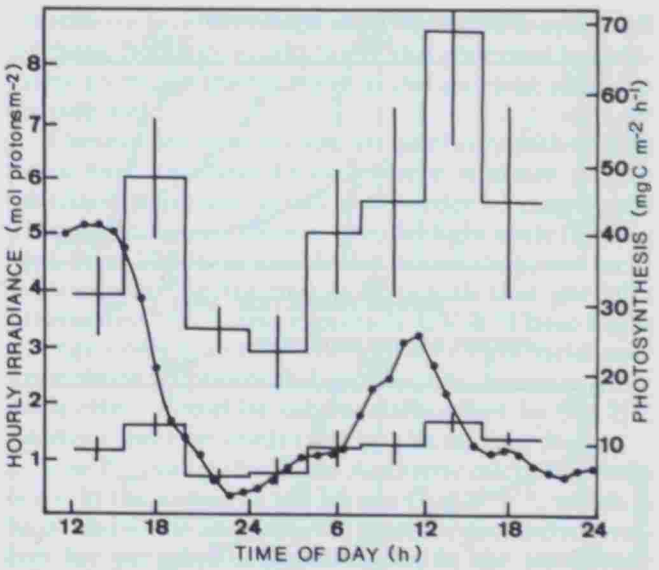

FIG. 6. The diel variation in photosynthetic rates for two oscillatoriacean mat communities incubated *in situ* over 21–22 January 1990: O8—Skua (top histogram) and O6–Fresh (bottom histogram). Each value is the mean for four replicate bottles ±2 SE. The irradiance curve (●) is for hourly totals in the waveband of 400–700 nm.

Photosynthesis

The P versus I assays for a range of community types showed considerable variation in P_{max} both per unit area (10–40 mg C·m^{-2}·h^{-1}) and per unit Chl *a* (0.05–0.3 mg C·mg Chl *a*$^{-1}$·h^{-1}; Table 3). All of the communities, however, achieved saturation at less than 15% of ambient midday irradiance (I_k values from 27 to 178 μmol·m^{-2}·s^{-1}; Table 3), and in these short-term incubations there was no evidence indicating photoinhibition even under full sunlight (Fig. 5). Thus, there was minimal change in photosynthetic rates across most of the tested range of irradiances.

A P versus I curve was also obtained for mat L3–Brack incubated upside-down with its blue-green bottom layer exposed to the light. This incubation series gave a twofold higher α and P_{max} in comparison to measurements of the same mat cores incubated with the orange surface facing upward, as in the pond (Fig. 5, Table 3). These results provide further evidence of the strong self-shading and light limitation, particularly for the deep-living populations.

The series of photosynthetic measurements over a 36-h period confirmed the relatively low responsiveness of these communities to major fluctuations in light (Fig. 6). Over the first 24 h of measurement, the ambient downwelling irradiance changed by about a factor of 10, but the community photosynthetic rates of O8–Skua and O6–Fresh varied by a factor of 2–3. The *in situ* water temperature of the ponds varied from 4° to 6° C over the period of measurements. Photosynthesis tracked the daily irradiance curve with a slight phase lag (<3 h) and a considerably dampened amplitude of variation.

Vertical profiles of oxygen and photosynthesis were measured with microelectrodes in two of the oscillatoriacean mat communities (Fig. 7). Oxygen concentrations were above air equilibrium in both of the mats, with the highest values (200–250% saturation) recorded 2–3 mm below the mat surface. The O7–Conophyton mat had an irregular surface topography and pigmentation, and there were substantial differences in the shape of the oxygen profiles only a few millimeters apart. Conical orange-brown structures up to 3 mm high were distributed across the otherwise flat, orange or orange-green (less common) regions of the mat. One of the cones was profiled, and it showed uniform oxygen concentrations at values slight above air equilibrium. In both the orange and the orange-green flat sections of the mat, the oxygen tensions increased with depth to in excess of 200% near the bottom of the profile;

TABLE 3. *Photosynthetic parameters for the mat P versus I curves as shown in Figure 5, but normalized to Chl* a. *Standard error is given in parentheses for each regression estimate of* α *and* P_{max}.

Mat community	P_{max} (μg C·(μg Chl *a*)$^{-1}$·h^{-1})	α (μg C·(mg Chl *a*)$^{-1}$·h^{-1}·(μmol photons·m^{-2}·s^{-1})$^{-1}$)	I_k (μmol photons·m^{-2}·s^{-1})
S3–SOS	0.048 (0.004)	0.3 (0.06)	178
L3–Brack	0.110 (0.002)	2.4 (0.2)	45
O10–Orange	0.135 (0.012)	1.4 (0.4)	97
O8–Skua	0.205 (0.007)	7.5 (1.0)	27
O6–Fresh	0.256 (0.010)	8.9 (1.8)	29
L3–Brack (inverted)	0.275 (0.007)	5.4 (0.5)	51

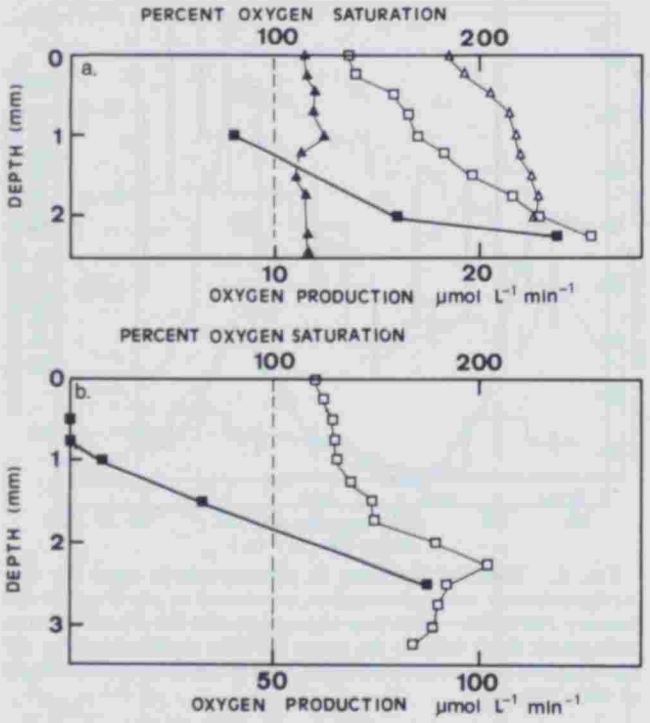

FIG. 7. Vertical profiles of oxygen concentration (□, expressed as % air equilibrium at 5° C) and photosynthetic oxygen production rates (■) in two oscillatoriacean mats, under clear sky conditions on 26 January 1990. Depth refers to distance from the upper mat surface. The measurements extended into but not to the bottom of the blue-green layer to prevent the breakage of the microelectrodes. a) O7–Conophyton; b) O8–Skua. The data for O7–Conophyton are for a flat orange section of the mat. Also plotted are oxygen concentration profiles within a 2-mm-high, orange cone (▲) and within a flat, orange-green section (△) of the O7–Conophyton mat.

this vertical gradient was much more pronounced in the orange mat (Fig. 7). In both O7–Conophyton (orange region) and O8–Skua, the photosynthetic oxygen production rates increased with increasing depth down the mat profile, consistent with the increased pigment as well as oxygen concentrations at depth (Fig. 7).

DISCUSSION

Nutrient supply seems unlikely to have been a major constraint on population growth rates in these microbial mat environments. The interstitial waters were rich in dissolved phosphorus (300 to >1000 mg DRP·m^{-3}), a condition that is likely to favor cyanobacterial growth (e.g. Pick and Lean 1987). The mats also contained several hundred milligrams of NH_4-N·m^{-3}, which may account for the dominance by nonheterocystous species despite the low inorganic N:P ratios. It is of interest that the analyses of ammonium and DRP in the overlying pond water provided no evidence of the nutrient-rich conditions inside the communities. It is possible that the mat-compression technique used here caused some cellular breakage and the release of intracellular nutrients. However, the mats contained very few metazoans (low concentrations of nematodes and rotifers) and were almost exclusively dominated by the cyanobacterial trichomes. If cellular breakage was a factor contributing to the measured N and P concentrations, then this also implies high concentrations of stored reserves and nutrient sufficiency rather than deficiency. The low nitrate concentrations yet high ammonium and oxygen indicated either a lack of nitrifier activity despite the apparently favorable substrate conditions or a tight coupling between nitrate production and loss processes within the mat.

As in the temperate zone, the oscillatoriacean communities in Antarctica show a strong differential production of light-screening and light-absorbing compounds down through the mat profile. The surface layer populations were enriched in carotenoids, which absorb maximally in the region of 400–550 nm. There were other components in the surface layer (perhaps contained within the thick mucilage) that attenuated UV radiation. For example, UV radiation was strongly absorbed to an increasing extent below 350 nm in the surface mucilage of L2–Green (Fig. 3b). A UV-A/B absorbing pigment has been isolated from terrestrial *Nostoc commune* at temperate latitudes (Scherer et al. 1988), and similar compounds may contribute to the UV-screening properties of the upper strata of Antarctic cyanobacterial mats. Mycosporine-like amino acids, compounds that absorb across the UV spectrum, are now known to occur in many species of cyanobacteria (Shibata 1969, Garcia-Pichel and Castenholz 1993).

The persistent decline in stratospheric ozone levels over Antarctica has generated increasing concern about the effects of UV-B radiation on the Antarctic biota, both directly and through the photochemical production of highly reactive oxidants (Karentz 1991, Vincent and Roy 1993). The UV-screening properties of Antarctic cyanobacterial mats coupled with the antioxidant activity of their carotenoids is likely to confer a high level of resistance to such effects. High carotenoid concentrations were recorded throughout the mat profiles, although highest concentrations per unit Chl *a* were in the surface layer. These compounds are known to play a variety of quenching roles (e.g. Jialal et al. 1991, Telfer et al. 1991) that may be especially important in the highly oxygenated mat environment, particularly where the rates of biosynthetic repair are slowed by the continuous near-freezing temperatures.

The subsurface community in these mats inhabited a deep euphotic regime of extreme shade. These lower strata were enriched in Chl *a* and phycocyanin, as evidenced by the absorbance maxima at 680 and 620 nm, respectively, and the distinct blue-green coloration. These pigments in the deep Chl *a* maximum (DCM) are likely to be especially effective in harvesting the red-dominated irradiance in the lower mat environment. In L2–Green, for example,

most of the Chl *a* was located in a DCM in the bottom 5 mm, where incoming visible irradiance was restricted to wavelengths of 550–670 nm at an irradiance of about 2% of incident radiation in the same waveband. The penetration of near infra-red radiation in this and other mats was undoubtedly beneficial to the purple sulfur bacteria. These organisms were especially prevalent at the base of those mats with an anaerobic, sulfidogenic underlayer.

It should be noted that our measurements of downwelling irradiance within the mat profiles are likely to have underestimated the true *in situ* photosynthetically available radiation. Microbial mats provide a highly scattering medium for light penetration, and backscattered light can substantially increase (up to a factor of 2) the absolute scalar irradiance, especially in the near-surface strata, and can also alter the spectral balance (e.g. Jorgensen and Des Marais 1988, Lassen et al. 1992).

A number of previous studies have drawn attention to the low assimilation numbers that characterize Antarctic cyanobacterial mats, and a variety of factors have been evaluated as potential explanations including freeze-damaged cells (Hawes 1989), nutrient limitation (Howard-Williams and Vincent 1989), low-temperature-depressed photosynthetic rates (Vincent and Howard-Williams 1989) and incompletely degraded, inactive forms of Chl *a* (Howard-Williams et al. 1990). The latter seems unlikely in the range of mats examined here, for we were unable to detect chlorophyllide *a*, phaeophytin *a*, or other related degradation products of Chl *a*. A more likely explanation based on the current set of observations is the physiological dominance of the mat by the DCM. The mat assimilation numbers are integral values for entire euphotic zones that are compressed into a few millimeters to centimeters and that are dominated by the community of deep-living shade populations. As such, they cannot be directly compared with, for example, planktonic values for discrete depths within the euphotic zone of a water column.

The combination of highest concentrations of photoprotective pigments per unit Chl *a* in the surface strata of mainly nonmigrating species and highest concentrations of light-harvesting pigments deep in the mats appears to allow the Antarctic cyanobacterial mats to achieve substantial rates of photosynthesis per unit area under variable ambient light conditions. The vertical migration capability of some of the deeper species with thick trichomes is likely to play a further adaptive role under the broad range of light conditions, from ice and snow cover to complete meltout, which characterize these Antarctic environments. The strong near-surface attenuation of high-energy wavelengths may account for the apparent lack of photoinhibition in the short-term infrared gas analyzer incubations as well as during the longer ^{14}C incubations over the 24-h cycle. The I_k value for the communities was well below ambient irradiance levels through most of the 24-h cycle. All of these features would favor the observed insensitivity to major fluctuations in the incident solar radiation field.

These observations contrast markedly with results from the Antarctic Ocean where summer phytoplankton populations can show order of magnitude changes in P_{max} and α over the diel light cycle (Rivkin and Putt 1987). It should be noted that our incubations were performed in glass vials that partially attenuated UV-A and especially UV-B. These high-energy components of the ambient light field may contribute to photoinhibition *in situ*; however, any such effect would be substantially offset by the UV photoprotection conferred by the surface layer.

The P_{max} values for these Antarctic microbial mats were in the range of 10–50 mg $C \cdot m^{-2} \cdot s^{-1}$, which is at or above the area-specific primary production values for periphyton communities in the temperate zone. For example, the epilithic cyanobacterial communities of five oligotrophic lakes in North America had *in situ* production rates ranging up to a maximum of 9 mg $C \cdot m^{-2} \cdot h^{-1}$ (Loeb and Reuter 1981). The standing crop of epilithic Chl *a* in the North American lakes was also much lower than in Antarctica, but the integral assimilation ratios were similar (e.g. 0.2 mg C·mg Chl $a^{-1} \cdot h^{-1}$ in Donner Lake, California), suggesting that the periphyton in temperate-latitude environments may share some of the ecophysiological attributes described here for Antarctic cyanobacteria. Our estimates overlap with those obtained by Boston and Hill (1991) for periphyton from a series of Tennessee streams where area-specific photosynthetic rates were 15-200 mg $C \cdot m^{-2} \cdot h^{-1}$ and integral assimilation ratios were 0.26–1.4 μg C·(μg Chl *a*)$^{-1} \cdot h^{-1}$. These authors noted the apparent shade characteristics of the periphytic P versus I curves (low P_{max} per unit Chl *a*, a high α, and thus a low I_k), and they suggested that this reflected the strong self-shading within the periphyton community. Most of the I_k values for the Antarctic mats were a factor of two to five times below those recorded in Tennessee, suggesting an extreme shade effect associated with the inverted photosynthetic profiles and the DCM dominance of community production.

Photosynthetic rates of at least an order of magnitude higher than in the Antarctic communities have been recorded in microbial mats from high-temperature waters—for example, 700–1800 μmol $O_2 \cdot L^{-1} \cdot min^{-1}$ in geothermal cyanobacteria-dominated mats (Ward et al. 1989, Castenholz et al. 1991) and up to 870 μmol $O_2 \cdot L^{-1} \cdot min^{-1}$ in the diatom and cyanobacterial communities in a solar-heated desert lake (cf. 88 μmol $O_2 \cdot L^{-1} \cdot min^{-1}$ in the Skua Pond mat using the same microelectrode technique). However, many other features that we observed in Antarctic microbial mats have been previously described in these warm-water communities—for example, photosynthetic maxima well below the mat

surface (e.g. Jorgensen et al. 1983, Ward et al. 1989), strong vertical gradients in light and oxygen (e.g. Castenholz et al. 1991), major shifts in pigment composition down through the profile (e.g. Palmisano et al. 1989), substantial mucilage production (e.g. Jorgensen et al. 1983), and trichome motility (Castenholz et al. 1991). Our observations from the south polar zone suggest that these same properties found under high-temperature conditions may also contribute to the adaptive success of cyanobacteria in extreme cold-water environments.

We thank Dr. Malcolm Macfarlane, Mr. David Geddes, and other staff of DSIR Antarctica, for logistic support; Dr. Steve de Mora's research team from the University of Auckland, for invaluable assistance in the field; VXE-6 Squadron of the United States Navy, for helicopter support; Lynell May, Liana Hrstich, and Maude Lecourt, for technical assistance; Dr. Beverley Pierson, for the loan of the LiCor scanning spectroradiometer; and FRST (New Zealand), NSF (U.S.A.), and NSERC (Canada), for funding support.

Aminot, A. & Kerouel, R. 1982. Dosage automatique de l'urée dans l'eau de mer: une méthode très sensible à la diacetylmonoxime. *Can. J. Fish. Aquat. Sci.* 39:174–83.

Boston, H. L. & Hill, W. R. 1991. Photosynthesis–light relations of stream periphyton communities. *Limnol. Oceanogr.* 36:644–56.

Broady, P. A 1986. Ecology and taxonomy of the terrestrial algae of the Vestfold Hills. *In* J. Pickard [Ed.] *Antactic Oasis Terrestrial Environments and History of the Vestfold Hills.* Academic Press, Australia, pp. 165–202.

Broady, P. A. & Kibblewhite, A. L. 1991. Morphological characterization of Oscillatoriales (Cyanobacteria) from Ross Island and southern Victoria Land, Antarctica. *Antactic Sci.* 3: 35–45.

Castenholz, R. W., Bauld, J. & Jorgensen, B. B. 1990. Anoxygenic microbial mats of hot springs: thermophilic *Chlorobium* sp. *FEMS Microbiol. Ecol.* 74:325–36.

Castenholz, R. W., Jorgensen, B. B., D'Amelio, E. & Bauld, J. 1991. Photosynthetic and behavioral versatility of the cyanobacterium *Oscillatoria boryana* in a sulfide-rich microbial mat. *FEMS Microbiol. Ecol.* 86:43–58.

Cohen, Y., Castenholz, R. W. & Halvorsen, H. O. 1984. The interdisciplinary approach to the study of microbial mats: perspectives for future research—discussion. *In* Cohen, Y., Castenholz, R. W. & Halvorsen, H. G. [Eds.] *Microbial Mats: Stromatolites.* Alan R. Liss, New York, pp. 471–7.

Downes, M. T. 1978. An automated method of low reactive phosphorus concentrations in natural waters in the presence of arsenic, silicon and mercuric chloride. *Water Res.* 12:743–5.

Garcia-Pichel, F. & Castenholz, R. W. 1993. Occurrence of UV-absorbing, mycosporine-like compounds among cyanobacterial isolates and an estimate of their screening capacity. *Appl. Environ. Microbiol.* 59:163–9.

Garrett, P. 1970. Phanerozoic stromatolites: non-competitive ecologic restriction by grazing and burrowing animals. *Science (Wash. D.C.)* 169:171–3.

Geitler, L. 1932. *Cyanophyceae.* Rabenhorst's Kryptogamenflora von Deutchland, Osterreich und der Schweiz, v. 14. Akad. Verlag, Leipzig.

Goldman, C. R., Mason, D. T. & Wood, B. J. B. 1963. Light injury and inhibition in Antarctic freshwater phytoplankton. *Limnol. Oceanogr.* 8:313–22.

——— 1972. Comparative limnology of two small lakes on Ross Island, Antarctica. *Ant. Res. Ser.* 20:1–20.

Hawes, I. 1989. Filamentous green algae in freshwater streams on Signy Island, Antarctica. *Hydrobiologia* 172:1–18.

Hawes, I. & Brazier, P. 1991. Freshwater stream ecosystems of James Ross Island, Antarctica. *Antarctic Sci.* 3:265–71.

Howard-Williams, C., Downes, M. T. & Vincent, W. F. 1989. Microbial biomass, photosynthesis and chlorophyll *a* related pigments in the ponds of the McMurdo Ice Shelf, Antarctica. *Antarctic Sci.* 1:125–31.

Howard-Williams, C., Pridmore, R. D., Broady, P. A. & Vincent, W. F. 1990. Environmental and biological variability in the McMurdo Ice Shelf ecosystem. *In* Kerry, K. R. & Hempel, G. [Eds.] *Antarctic Ecosystems, Ecological Change and Conservation.* Springer-Verlag, New York, pp. 23–31.

Howard-Williams, C. & Vincent, W. F. 1989. Microbial communities in southern Victoria Land streams (Antarctica) I. Photosynthesis. *Hydrobiologia* 172:27–38.

Jialal, J., Norkus, E. P., Cristol, L. & Grundy, S. M. 1991. β-carotene inhibits the oxidative modification of low-density lipoprotein. *Biochem. Biophys. Acta* 1086:134–8.

Jorgensen, B. B. & Des Marais, D. J. 1988. Optical properties of benthic photosynthetic communities: fiber optic studies of cyanobacterial mats. *Limnol. Oceanogr.* 33:99–113.

Jorgensen, B. B., Revsbech, N. P. & Cohen, Y. 1983. Photosynthesis and structure of benthic microbial mats: microelectrode and SEM studies of four cyanobacterial communities. *Limnol. Oceanogr.* 28:1075–93.

Karentz, D. 1991. Ecological considerations of Antarctic ozone depletion. *Antarctic Sci.* 3:3–11.

Lassen, C., Ploug, H. & Jorgensen, B. B. 1992. Microalgal photosynthesis and spectral scalar irradiance in coastal marine sediments of Limfjorden, Denmark. *Limnol. Oceanogr.* 37: 760–72.

Loeb, S. L. & Reuter, J. 1981. The epilithic periphyton community: a five lake comparative study of community productivity, nitrogen metabolism and depth distribution of standing crop. *Verh. Int. Verein. Limnol.* 21:346–52.

Mantoura, R. F. C. & Llewellyn, C. A. 1983. The rapid determination of algal chlorophyll and carotenoid pigments and their breakdown products in natural waters by reverse-phase high performance liquid chromatography. *Anal. Chim. Acta* 151:297–314.

Nydahl, F. 1976. On the optimal conditions for the reduction of nitrate to nitrite by cadmium. *Talanta* 23:349–57.

Oguni, A., Tanaka, Y., Uemura, M., Yamamoto, M. & Takahashi, E. 1987. Floristic studies on algae from inland waters of Ongul Islands and vicinity, Antarctica I. East Ongul Island. *Proc. NIPR Symp. Polar Biol.* 1:233–54.

Palmisano, A. C., Summons, R. E., Cronin, S. E. & Des Marais, D. J. 1989. Lipophilic pigments from cyanobacterial (blue-green algal) and diatom mats in Hamelin Pool, Shark Bay, Western Australia. *J. Phycol.* 25:655–61.

Pick, F. R. & Lean, D. R. S. 1987. The role of macronutrients in controlling cyanobacterial dominance in temperate lakes. *N.Z. J. Mar. Freshwater Res.* 21:425–34.

Priddle, J. 1980. The production ecology of benthic plants in some Antarctic lakes I. In situ production studies. *J. Ecol.* 68: 141–66.

Rivkin, R. & Putt, M. 1987. Diel periodicity of photosynthesis in polar phytoplankton: influence on primary production. *Science (Wash. D.C.)* 238:1285–8.

Scherer, S., Chen, T. W. & Böger, P. 1988. A new UV-A/B protecting pigment in the terrestrial cyanobacterium *Nostoc commune. Plant Physiol.* 88:1055–7.

Shibata, K. 1969. Pigments and a UV-absorbing substance in corals and a blue-green alga of the Great Barrier Reef. *Plant Cell Physiol.* 10:325–35.

Solorzano, L. 1969. Determination of ammonia in natural waters by the phenolhypochlorite method. *Limnol. Oceanogr.* 14:799–801.

Telfer, A., Rivas, J. D. L. & Barber, J. 1991. β-carotene within the isolated photosystem II reaction centre: photo-oxidation and irreversible bleaching of this chromophore by oxidised P680. *Biochem. Biophys. Acta* 1060:106–14.

Vincent, W. F. 1988. *Microbial Ecosystems of Antarctica.* Cambridge University Press, Cambridge, 304 pp.

Vincent, W. F., Downes, M. T., Castenholz, R. W. & Howard-Williams, C. 1993. Community structure and pigment or-

ganisation of cyanobacteria-dominated microbial mats in Antarctica. *Eur. J. Phycol.* 28:(in press).
Vincent, W. F. & Howard-Williams, C. 1986. Antarctic stream ecosystems: physiological ecology of a blue-green algal epilithon. *Freshwater Biol.* 16:219–33.
——— 1989. Microbial communities in southern Victoria Land streams (Antarctica) II. The effects of low temperature. *Hydrobiologia* 172:39–49.
Vincent, W. F. & Roy, S. 1993. Solar ultraviolet-B radiation and aquatic primary production: damage, protection and recovery. *Environ. Rev.* 1:1–12.
Ward, D. M., Weller, R. Shiea, J., Castenholz, R. W. & Cohen, Y. 1989. Hot spring microbial mats: anoxygenic and oxygenic mats of possible evolutionary significance. *In* Cohen, Y. & Rosenberg, E. [Eds.] *Microbial Mats: Physiological Ecology of Benthic Microbial Communities.* American Society of Microbiology, Washington, D.C., pp. 3–15.
Webb, W. L., Newton, M. & Starr, D. 1974. Carbon dioxide exchange of *Alnus rubra*: a mathematical model. *Oecologica* 17:281–91.
Webster, J. G., Brown, K. L. & Vincent, W. F. 1994. Geochemical processes affecting meltwater chemistry and the formation of saline brines in the Victoria Valley and Bull Pass region, Antarctica. *Hydrobiologia* (in press).
Wharton, R. A., Parker, B. C. & Simmons, G. M. 1983. Distribution, species composition and morphology of algal mats (stromatolites) in Antarctic dry valley lakes. *Phycologia* 22: 355–65.

J. Phycol. **29,** 755–766 (1993)

RESPONSE OF THE PHOTOSYNTHETIC APPARATUS OF *PHAEODACTYLUM TRICORNUTUM* (BACILLARIOPHYCEAE) TO NITRATE, PHOSPHATE, OR IRON STARVATION[1]

Richard J. Geider[2]

College of Marine Studies, University of Delaware, Lewes, Delaware 19958-1298

and

Julie La Roche, Richard M. Greene, and Miguel Olaizola[3]

Oceanographic & Atmospheric Sciences Division, Brookhaven National Laboratory, Upton, New York 11973

ABSTRACT

The effects of nitrate, phosphate, and iron starvation and resupply on photosynthetic pigments, selected photosynthetic proteins, and photosystem II (PSII) photochemistry were examined in the diatom Phaeodactylum tricornutum *Bohlin (CCMP1327). Although cell chlorophyll* a *(chl* a*) content decreased in nutrient-starved cells, the ratios of light-harvesting accessory pigments (chl* c *and fucoxanthin) to chl* a *were unaffected by nutrient starvation. The chl* a*-specific light absorption coefficient* ($\overline{a^*}$) *and the functional absorption cross-section of PSII* (σ) *increased during nutrient starvation, consistent with reduction of intracellular self-shading (i.e. a reduction of the "package effect") as cells became chlorotic. The light-harvesting complex proteins remained a constant proportion of total cell protein during nutrient starvation, indicating that chlorosis mirrored a general reduction in cell protein content. The ratio of the xanthophyll cycle pigments diatoxanthin and diadinoxanthin to chl* a *increased during nutrient starvation. These pigments are thought to play a photoprotective role by increasing dissipation of excitation energy in the pigment bed upstream from the reaction centers. Despite the increase in diatoxanthin and diadinoxanthin, the efficiency of PSII photochemistry, as measured by the ratio of variable to maximum fluorescence* (F_v/F_m) *of dark-adapted cells, declined markedly under nitrate and iron starvation and moderately under phosphate starvation. Parallel to changes in* F_v/F_m *were decreases in abundance of the reaction center protein D1 consistent with damage of PSII reaction centers in nutrient-starved cells. The relative abundance of the carboxylating enzyme, ribulose bisphosphate carboxylase/oxygenase (RUBISCO), decreased in response to nitrate and iron starvation but not phosphate starvation. Most marked was the decline in the abundance of the small subunit of RUBISCO in nitrate-starved cells. The changes in pigment content and fluorescence characteristics were typically reversed within 24 h of resupply of the limiting nutrient.*

Key index words: absorption cross-section; Bacillariophyceae; diadinoxanthin; diatoxanthin; fluorescence quenching; fucoxanthin–chlorophyll–protein complex; nutrient limitation; Phaeodactylum tricornutum; *reaction center II; western blot*

Because growth is a major sink for photosynthate, the reduction of growth rate by nutrient limitation is expected to affect the composition and functioning of the photosynthetic apparatus. Of all the macro- and micronutrients essential for marine algal growth, nitrogen, phosphorus, and iron have been postulated as possible limiting factors in the oceans. Although the ultimate effect of nutrient limitation is a reduction in photosynthesis and growth, the

[1] Received 5 April 1993. Accepted 23 August 1993.
[2] Address for reprint requests.
[3] Present address: Institute for Remote Sensing Applications, Joint Research Center, I-21020, Ispra (VA), Italy.